Adaptive Dead-beat Sliding Plane Multivariable Decoupled Control of a Microgrid

Eduardo Giraldo

Abstract—**This work proposes a multivariable decoupled adaptive control of a microgrid based on a sliding plane approach. The proposed method is designed by considering a discrete-time reaching law and the dead-beat sliding plane where the controller and a state-space model use plant parameters given by an online digital identifier. In addition, a digital integrator is used to reduce the tracking error. It is worth noting that the dead-beat control is obtained by forcing the system dynamics in the sliding plane. The proposed approach is applied over a multivariable microgrid described by a transfer matrix. The proposed method is evaluated over a simulated microgrid using a digital implementation of the proposed adaptive controller under noiseless and additive noise conditions. The proposed approach is also evaluated in real-time by considering a Hardware-In-the-Loop structure. To this end, a Texas Instruments C2000 Delfino processor is used. The performance of the proposed approach is evaluated in terms of tracking error, settling-time, and robustness to external disturbances. In addition, the proposed approach is compared to polynomial controllers by using a pole-placement approach.**

Index Terms—**Dead-beat, sliding mode control, real-time, microgrid.**

I. Introduction

THE sliding mode control approach for multivariable systems has been used for many years as a successful technique to obtain stability and fast-tracking response, especially for systems with high frequency switching capabilities [1], [2], [3], [4], [5]. This control approach has been applied for multivariable systems, especially by considering a state-space sliding mode observer for sensorless-based control [6], [7], [8]. Multivariable controllers are usually designed to evaluate some range in parameter variations. When these are out of range, the control behaves poorly, yielding undesirable responses [6]. Therefore, parameter identification is needed to improve the system's behavior, resulting in a robust control approach [9].

Microgrids are the current standard description used to refer to many systems that involve interconnected subsystems that includes but are not limited to DC-DC converters and renewable energy resources such as photo-voltaic panels and wind energy generators, among others [10]. In [11], a HIL structure for evaluation of control systems is proposed based on C2000 microcontrollers [12]. In [13], a decoupled multivariable control for a large-scale microgrid is proposed based on an embedded control where the evaluation is performed in a Hardware-In-the-Loop (HIL) structure.

Manuscript received January 25, 2022; revised October 3, 2022. This work is funded by project no. 6-22-8 entitled "Identificación y control de sistemas multivariables interconectados a gran escala" by Universidad Tecnológica de Pereira, Pereira, Colombia.

Eduardo Giraldo is a full professor at the Department of Electrical Engineering, Universidad Tecnológica de Pereira, Pereira, Colombia. Research group in Automatic Control. E-mail: egiraldos@utp.edu.co

A dead-beat controller is a common technique to obtain fast-tracking reference responses. In [14], a higher-order sliding dead-beat control is proposed to get a fast-tracking reaction for multivariable linear systems. In [15], an adaptive digital controller based on a dead-beat approach is designed for a linear third-order plant and validated over an analog simulation using an analog computer. In [16], a dead-beat observer is proposed for flux and torque control. It is noticeable that sliding mode control methods with dead beat dynamics result in a reliable and robustness control strategy compared to the standard pole-placement approach.

In this work, an adaptive multivariable decoupled control technique based on a sliding mode control is proposed. The proposed controller uses some incremental state variables, which tend to zero as the origin of the sliding plane is approached. An online digital parameter identifier provides the plant parameters to the controller and a state model. The controller uses a digital reaching law representing the sliding plane's reaching dynamics. The sliding plane, calculated online using the identified plant parameters, is designed in such a way that the closed-loop poles of the system are placed in the Z-plane origin to obtain dead-beat control in sliding mode [17]. In addition, a digital integrator is included in the system to reduce the steady-state tracking error. The proposed approach is evaluated in simulation under noiseless and additive noise conditions. Moreover, the proposed approach is evaluated over a real time environment by using a HIL structure. It is worth mentioning that the proposed approach is compared to state-of-the-art methods that considers state feedback by using eigen structure assignment. The real-time evaluation is performed over a Texas Instruments C2000 F28379D Delfino processor. The comparison of the methods is developed in terms of tracking error, settling time and robustness to external disturbances. The paper is organized as follows: in section II are presented the standardized microgrid model in discrete transfer matrix form, the adaptive decoupled control for each microgrid subsection, and the dead-beat approach for closed-loop dynamics. In section III is presented the identification and closed-loop control results for tracking reference over a simulated and a HIL real-time implementation, and in section IV are presented the conclusions and final remarks.

II. Theoretical framework

A. Microgrid model

In this work is proposed a microgrid system described by a transfer matrix defined as

$$Y(z) = H(z)U(z) \tag{1}$$

being

$$Y(z) = \begin{bmatrix} Y_1(z) \\ \vdots \\ Y_p(z) \end{bmatrix} \tag{2}$$

and

$$U(z) = \begin{bmatrix} U_1(z) \\ \vdots \\ U_q(z) \end{bmatrix} \tag{3}$$

and

$$H(z) = \begin{bmatrix} H_{11}(z) & \cdots & H_{1q}(z) \\ \vdots & & \\ H_{p1}(z) & \cdots & H_{pq}(z) \end{bmatrix} \tag{4}$$

the microgrid transfer matrix model in discrete time.

In this work, a decoupled controller is proposed based on a linear third-order approximated plant defined by

$$\frac{Y_i(z)}{U_j(z)} = \frac{z^{-1}(p_6 + p_5 z^{-1} + p_4 z^{-2})}{1 - p_1 z^{-1-p_2 z^{-2} - p_3 z^{-3}}} \tag{5}$$

where $p_1, p_2, \ldots, p_6$ are plant parameters, $Y_i(z)$ and $U_j(z$ are the output and the control variable, respectively.

The corresponding DARMA model of the microgrid [17] of (5) is:

$$\begin{aligned} y_i[k] =& p_1 y_i[k-1] + p_2 y_i[k-2] + p_3 y_i[k-3] \\ &+ p_4 u_j[k-3] + p_5 u_j[k-2] + p_6 u_j[k-3] \end{aligned} \tag{6}$$

where the actual output variable, $y_i[k]$, is expressed in terms of the past values of y_i and u_j.

B. Adaptive Sliding Mode Controller

The parameters of (6) are the unknown parameters model and are the ones the identifier should estimate in real-time. It is worth noting that the controller has computed in the function of the (6) parameters, resulting in an adaptive sliding mode controller.

The DARMA model of (6) can be expressed in the following way:

$$y_i[k] = \phi_i[k-1]^T \theta_0 \tag{7}$$

where

$$\phi_i[k-1] = \begin{bmatrix} y_i[k-1] \\ y_i[k-2] \\ y_i[k-3] \\ u_j[k-3] \\ u_j[k-2] \\ u_j[k-1] \end{bmatrix} \tag{8}$$

is a vector which contains the past values of y_i and u_j, and

$$\theta_0 = \begin{bmatrix} p_1 \\ p_2 \\ p_3 \\ p_4 \\ p_5 \\ p_6 \end{bmatrix} \tag{9}$$

is the unknown parameter vector that can be identified in real time by considering the least-square algorithm for parameter identification proposed in [9].

By using the identified parameters, an observer type state model is implemented:

$$\begin{bmatrix} x_1[k+1] \\ x_2[k+1] \\ x_3[k+1] \end{bmatrix} = \begin{bmatrix} p_1 & 1 & 0 \\ p_2 & 0 & 1 \\ p_3 & 0 & 0 \end{bmatrix} \begin{bmatrix} x_1[k] \\ x_2[k] \\ x_3[k] \end{bmatrix} + \begin{bmatrix} p_6 \\ p_5 \\ p_4 \end{bmatrix} u[k] \tag{10}$$

where $x_1[k] = y_i[k]$ is the output directly measured.

The adaptive controller uses the identified parameter vector θ at sample k, and the state variables, as follows:

$$\begin{aligned} \hat{x}_1[k] &= r[k] - x_1[k] \\ \Delta x_2[k] &= x_2[k] - x_2[k-1] \\ \Delta x_3[k] &= x_3[k] - x_3[k-1] \\ \Delta x_4[k] &= x_4[k] - x_4[k-1] \end{aligned} \tag{11}$$

These variables are zero when the system reaches a steady-state. A digital integrator is used to measure that the error $\hat{x}_1$ approaches zero in a regulator system, which adds a new state equation.

$$x_4[k+1] = x_4[k] + T\hat{x}_1[k] \tag{12}$$

where T is the discretization or sample time.

In this way the sliding plane:

$$s[k] = \hat{x}_1[k] + c_2 \Delta x_2[k] + c_3 \Delta x_3[k] + c_4 \Delta x_4[k] \tag{13}$$

is zero in the equilibrium state.

A necessary and sufficient condition to assure both sliding motion and convergence onto the sliding plane for discrete-time systems, as proposed in [18], [19], [20], is described as follows:

$$|s[k+1]| = |s[k]| \tag{14}$$

where the reaching conditions are defined when $s[k] > 0$ as

$$-s[k] < s[k+1] < s[k] \tag{15}$$

and when $s[k] < 0$ as

$$s[k] < s[k+1] < -s[k] \tag{16}$$

Therefore, the control variable can be chosen such that:

$$s[k+1] = K_s s[k] \tag{17}$$

with $-1 < K_s < 1$.

Equation (17) can be considered a reaching law for digital systems, representing the reaching dynamics to the sliding plane. By transforming (17) into the Z domain, the following equation is obtained:

$$S(z) = \frac{z}{z - K_s} s(0) \tag{18}$$

From the Z transform theory is is shown that if $0 \leq K_s < 1$ then the reaching dynamics is damped, and when $-1 < K_s \leq 0$ is under-damped. Therefore, a good choice for K_s is:

$$0 \leq K_s < 1 \tag{19}$$

In this way, out of the sliding plane, $u[k]$ can be chosen in such a way that (17) and (19) be satisfied.

As:

$$x_1[k] = r[k] - \hat{x}_1[k] \tag{20}$$

from (10) and (12) the following equations are obtained:

$$x_2[k+1] = p_2 r[k] - p_2 \hat{x}_1[k] + x_3[k] + p_5 u[k] \quad (21)$$

$$x_3[k+1] = p_3 r[k] - p_3 \hat{x}_1[k] + p_4 u[k] \quad (22)$$

$$x_4[k+1] = x_4[k] + T x_1[k] \quad (23)$$

from where:

$$\Delta x_2[k+1] = p_2 \Delta r[k] - p_2 \Delta \hat{x}_1[k] + \Delta x_3[k] + p_5 \Delta u[k] \quad (24)$$

$$\Delta x_3[k+1] = p_3 \Delta r[k] - p_3 \Delta \hat{x}_1[k] + p_4 \Delta u[k] \quad (25)$$

$$\Delta x_4[k+1] = \Delta x_4[k] + T \Delta \hat{x}_1[k] \quad (26)$$

From (12), it can be seen that

$$\hat{x}_1[k-1] = \frac{\Delta x_4[k]}{T} \quad (27)$$

and replacing (27) in (24), and considering that $\Delta r[k] = 0$ for a regulator system, the following equations are obtained:

$$\Delta x_2[k+1] = -p_2 \hat{x}_1[k] + \Delta x_3[k] + \frac{p_2}{T} \Delta x_4[k] + p_5 \Delta u[k] \quad (28)$$

$$\Delta x_3[k+1] = -p_3 \hat{x}_1[k] + \frac{p_3}{T} \Delta x_4[k] + p_4 \Delta u[k] \quad (29)$$

$$\Delta x_4[k+1] = T \hat{x}_1[k] \quad (30)$$

From (10):

$$\Delta x_1[k+1] = p_1 \Delta x_1[k] + \Delta x_2[k] + p_6 \Delta u[k] \quad (31)$$

and replacing (31) in

$$\hat{x}_1[k+1] - \hat{x}_1[k] = \Delta r[k+1] - \Delta x_1[k+1] \quad (32)$$

the following equation is obtained

$$\begin{aligned} \hat{x}_1[k+1] - \hat{x}_1[k] =& \Delta r[k+1] - p_1 \Delta x_1[k] \\ & - \Delta x_2[k] - p_6 \Delta u[k] \end{aligned} \quad (33)$$

As:

$$\Delta x_1[k] = \Delta r[k] - [\hat{x}_1[k] - \hat{x}_1[k-1]] \quad (34)$$

using (34), with $\Delta r[k+1] = \Delta r[k] = 0$ for a regulator system and (20), then:

$$\begin{aligned} \hat{x}_1[k+1] - \hat{x}_1[k] =& p_1 \hat{x}_1[k] - \Delta x_2[k] \\ & - \frac{p_1}{T} \Delta x_4[k] - p_6 \Delta u[k] \end{aligned} \quad (35)$$

As:

$$\begin{aligned} s[k+1] =& \hat{x}_1[k+1] + c_2 \Delta x_2[k+1] \\ & + c_3 \Delta x_3[k+1] + c_4 \Delta x_4[k+1] \end{aligned} \quad (36)$$

Replacing (35) and (28) in (36):

$$\begin{aligned} s[k+1] =& (Q+1)\hat{x}_1[k] - \Delta x_2[k] \\ & + c_2 \Delta x_3[k] + \left(c_4 - \frac{Q}{T} \right) \Delta x_4[k] + K_u \Delta u[k] \end{aligned} \quad (37)$$

where

$$Q = p_1 - c_2 p_2 - c_3 p_3 + c_4 T \quad (38)$$

$$K_u = -p_6 + c_2 p_5 + c_3 p_4 \quad (39)$$

Selecting

$$\Delta u[k] = -(F_1 \hat{x}_1[k] + F_2 \Delta x_2[k] + F_3 \Delta x_3[k] + F_4 \Delta x_4[k]) \quad (40)$$

and with (40) and (37) and using (17):

$$\begin{aligned} s[k+1] - K_s s[k] =& (Q + 1 - K_s - K_u F_1)\hat{x}_1[k] \\ & - (1 + K_s c_2 + K_u F_2)\Delta x_2[k] \\ & + (c_2 - K_s c_3 - K_u F_3)\Delta x_3[k] \\ & - \left(\frac{Q}{T} - c_4 + K_s c_4 + K_u F_4 \right) \\ & = 0 \end{aligned} \quad (41)$$

Thus the following control gains are obtained [15]:

$$F_1 = \frac{Q + 1 - K_s}{K_u} \quad (42)$$

$$F_2 = -\frac{1 + K_s c_2}{K_u} \quad (43)$$

$$F_3 = \frac{c_2 - K_s c_3}{K_u} \quad (44)$$

$$F_4 = \frac{1}{K_u} \left[-\frac{Q}{T} + (1 - K_s) c_4 \right] \quad (45)$$

C. Dead-beat approach

The coefficients c_2, c_3 and c_4, which are functions of the identified plant parameters, are calculated in real-time using a dead-beat approach. for the system to be stable when the $s[k] = 0$ plane is reached. Dead-beat dynamics in the sliding plane guarantee stability

With $s[k] = 0$, and from (13):

$$\hat{x}_1[k] = -c_2 \Delta x_2[k] - c_3 \Delta x_3[k] - c_4 \Delta x_4[k] \quad (46)$$

Replacing (46) in (37) and with $s[k+1] = 0$, in the sliding plane, the effective value of the control variable is found:

$$\Delta u^*[k] = K_{x_2} \Delta x_2[k] + K_{x_3} \Delta x_3[k] + K_{x_4} \Delta x_4[k] \quad (47)$$

where

$$\begin{aligned} K_{x_2} &= \frac{c_2(Q+1) + 1}{K_u} \\ K_{x_3} &= \frac{c_3(Q+1) - c_2}{K_u} \\ K_{x_4} &= \frac{Q(c_4 + \frac{1}{T})}{K_u} \end{aligned} \quad (48)$$

By defining:

$$A = \begin{bmatrix} a_{11} & a_{12} & a_{13} \\ a_{21} & a_{22} & a_{23} \\ a_{31} & a_{32} & a_{33} \end{bmatrix}, \Delta \bar{x}[k] = \begin{bmatrix} \Delta x_2[k] \\ \Delta x_3[k] \\ \Delta x_4[k] \end{bmatrix} \quad (49)$$

With (46) and (47) in (28):

$$\Delta \bar{x}[k+1] = A \Delta \bar{x}[k] \quad (50)$$

where

$$\begin{aligned} a_{11} &= p_2c_2 + p_5K_{x_2} \\ a_{12} &= 1 + p_2c_3 + p_5K_{x_3} \\ a_{13} &= p_2\left(c_4 + \frac{1}{T}\right) + p_5K_{x_4} \\ a_{21} &= p_3c_2 + p_4K_{x_2} \\ a_{22} &= p_3c_3 + p_4K_{x_3} \\ a_{23} &= p_3\left(c_4 + \frac{1}{T}\right) + p_4K_{x_4} \\ a_{31} &= -c_2T \\ a_{32} &= -c_3T \\ a_{33} &= -c_4T \end{aligned} \tag{51}$$

The eigenvalues of A govern the system stability in the sliding plane. Therefore, if the closed-loop poles are placed in the Z plane origin, excellent stability is assured, as described in [15]. Therefore:

$$\det(zI - A) = z^3 \tag{52}$$

Then

$$\begin{bmatrix} b_{11} & b_{12} & b_{13} \\ b_{21} & b_{22} & b_{23} \\ b_{31} & b_{32} & b_{33} \end{bmatrix} = \begin{bmatrix} c_2 \\ c_3 \\ c_4 \end{bmatrix} = \begin{bmatrix} p_5 \\ p_4 \\ 0 \end{bmatrix} \tag{53}$$

where

$$\begin{aligned} b_{11} &= p_2p_6 - p_1p_5 - p_5 + p_4 \\ b_{21} &= p_3p_6 - p_2p_6 - p_1p_4 - p_4 + p_1p_5 \\ b_{31} &= p_1p_4 - p_3p_6 \\ b_{12} &= p_3p_6 - p_1p_4 - p_4 \\ b_{22} &= -p_3p_6 + p_3p_5 - p_2p_4 + p_1p_4 \\ b_{32} &= p_2p_4 - p_3p_5 \\ b_{13} &= -p_6T \\ b_{23} &= -p_5T \\ b_{33} &= -p_4T \end{aligned} \tag{54}$$

By solving (53) the sliding plane coefficients are obtained, and thus, global stability is assured with a dead-beat approach dynamics [15].

III. Results

The proposed adaptive control approach based on identification and dead-beat stability design, is evaluated over a microgrid with 3 inputs and 3 outputs, as defined in [13] with a sampling time $T = 0.5$ milliseconds. The system is evaluated in simulation and in a HIL structure for real time results. Three segments of the microgrid are analyzed according to [13], being the output vector $Y(z)$ defined as

$$Y(z) = \begin{bmatrix} V_1(z) \\ V_2(z) \\ V_3(z) \end{bmatrix} \tag{55}$$

being $V_j(z)$ for $j = 1, 2, 3$ the voltage output at the coupling nodes, and the input vector $U(z)$ defined as

$$U(z) = \begin{bmatrix} V_{d1}(z) \\ V_{d2}(z) \\ V_{d3}(z) \end{bmatrix} \tag{56}$$

being V_{dj} with $j = 1, 2, 3$ the inputs of the microgrid which are the voltage output of the DC-DC converters. In addition, the transfer matrix $H(z)$ related to $Y(z) = H(z)U(z)$ is obtained in discrete-time, where the corresponding discrete transfer function are defined as follows:

$$H_{11}(z) = \frac{-2.5}{(z + 48.95)(z - 0.8999)} \tag{57}$$

$$H_{21}(z) = 0 \tag{58}$$

$$H_{31}(z) = 0 \tag{59}$$

$$H_{12}(z) = \frac{-6.25}{(z + 48.95)^2(z^2 - 1.8z + 0.8098)} \tag{60}$$

$$H_{22}(z) = \frac{-2.5}{(z + 48.95)(z - 0.8999)} \tag{61}$$

$$H_{32}(z) = 0 \tag{62}$$

$$H_{13}(z) = \frac{-15.625}{(z + 48.95)^3(z - 0.8999)^2(z - 0.95)} \tag{63}$$

$$H_{23}(z) = \frac{-6.25}{(z + 48.95)^2(z - 0.95)(z - 0.8999)} \tag{64}$$

$$H_{33}(z) = \frac{-2.5}{(z + 49)(z - 0.95)} \tag{65}$$

In Fig. 1 is depicted the simulation of the microgrid system.

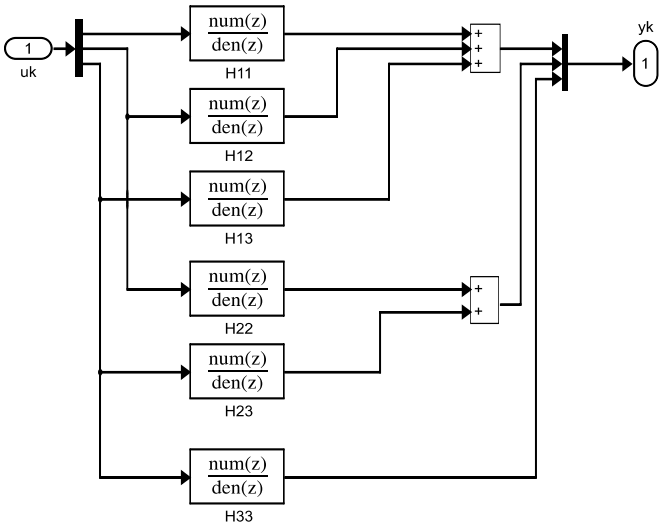

Fig. 1. Schematic diagram of the microgird simulation based on (57)

It is worth noting that the transfer functions $H_{ii}(z)$ for $i = 1, 2, 3$ are defined as second-order transfer functions. However, in order to include into the identified model the dynamics related to the coupling of the $H_{ii}(z)$ transfer function with the other microgrid subsystems, a higher-order system for (6) is assumed for system identification (in this case, a third-order system).

The closed loop diagram by including the proposed adaptive control approach is shown in Fig. 2. It is worth mentioning that the identification stage is used to design the controller coefficients according to (54).

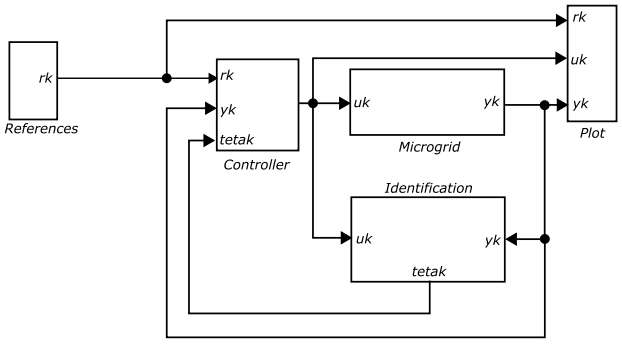

Fig. 2. Schematic diagram of the proposed adaptive control approach

A comparison analysis of the performance of the proposed approach is performed by using a pole placement technique with a dead beat closed-loop dynamics for a classical polynomial controller. In Fig. 3 is presented the output response v_1 for reference tracking by using a pole placement technique with dead beat closed loop dynamics.

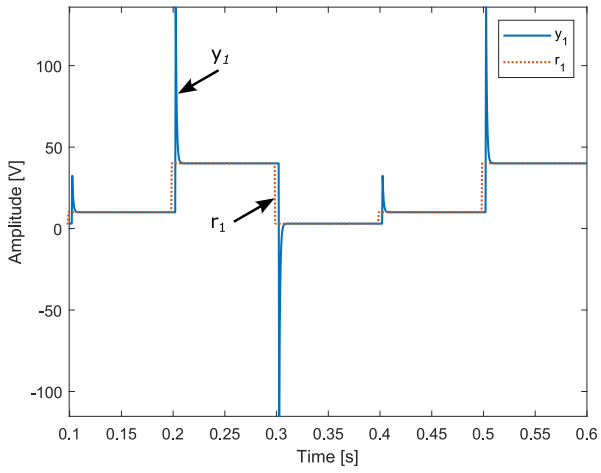

Fig. 3. Output v_1 considering reference tracking in the microgrid for a closed loop dead beat polynomial controller

In Fig. 4 is presented the control signal for reference tracking response shown in Fig. 3.

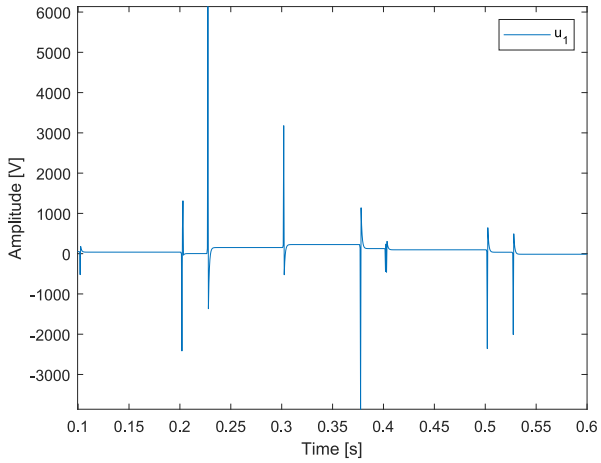

Fig. 4. Control signal for transfer function H_{11} of the microgrid

In Fig. 5 is presented the output response v_2 for reference tracking by using a pole placement technique with dead beat closed loop dynamics.

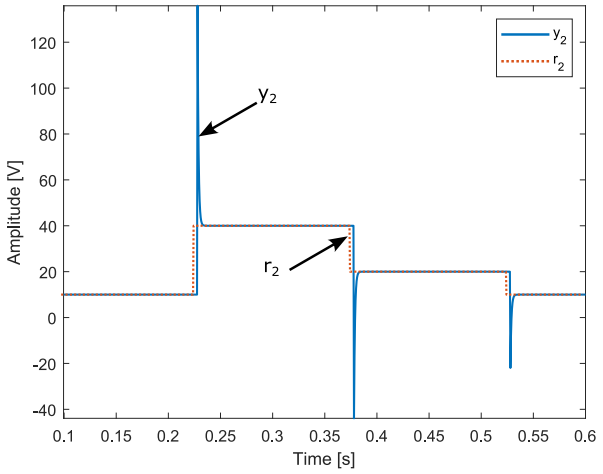

Fig. 5. Output v_2 considering reference tracking in the microgrid for a closed loop dead beat polynomial controller

In Fig. 6 is presented the control signal for reference tracking response shown in Fig. 5.

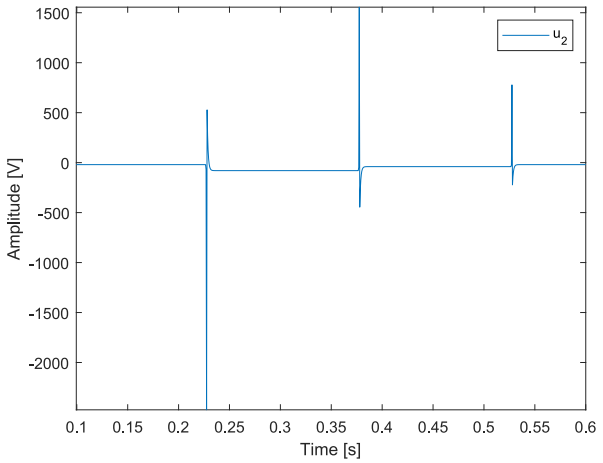

Fig. 6. Control signal for transfer function H_{22} of the microgrid

In Fig. 7 is presented the output response v_3 for reference tracking by using a pole placement technique with dead beat closed loop dynamics.

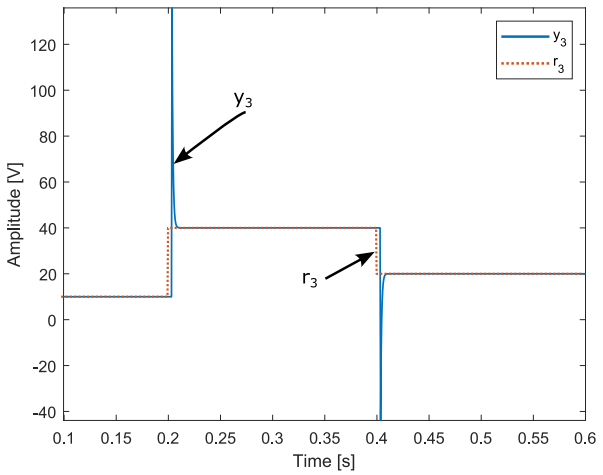

Fig. 7. Output v_3 considering reference tracking in the microgrid for a closed loop dead beat polynomial controller

In Fig. 8 is presented the control signal for reference tracking response shown in Fig. 7.

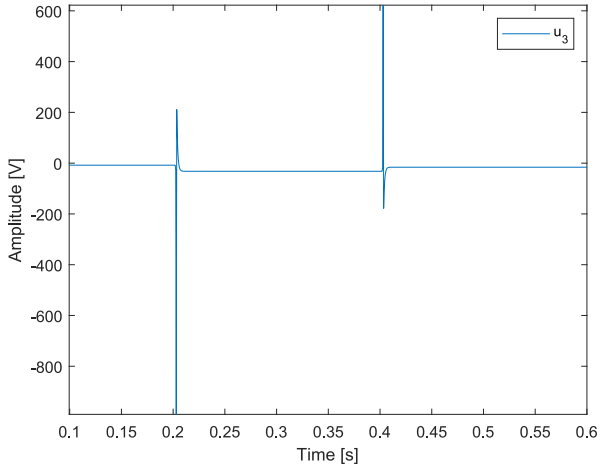

Fig. 8. Control signal for transfer function H_{33} of the microgrid

A similar evaluation is performed under noise conditions. In Fig. 9 is presented the tracking response of the first segment of the microgrid under noise conditions.

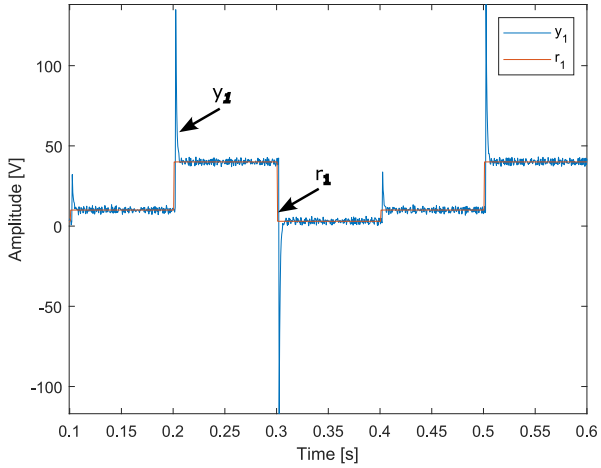

Fig. 9. Output v_1 tracking response of the first segment of the microgrid under noise conditions

In Fig. 10 is presented the tracking response of the second segment of the microgrid under noise conditions.

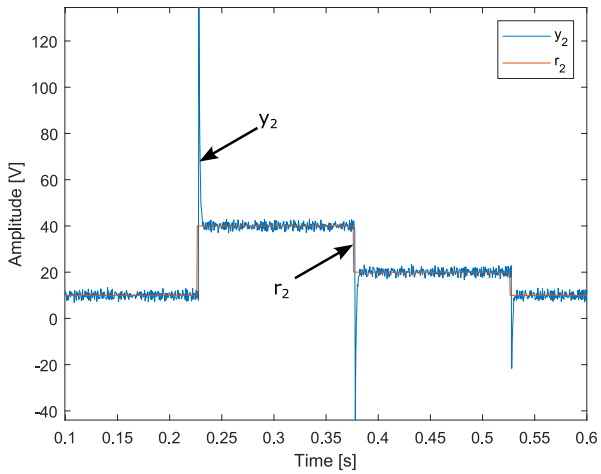

Fig. 10. Output v_2 tracking response of the second segment of the microgrid under noise conditions

In Fig. 11 is presented the tracking response of the third segment of the microgrid under noise conditions.

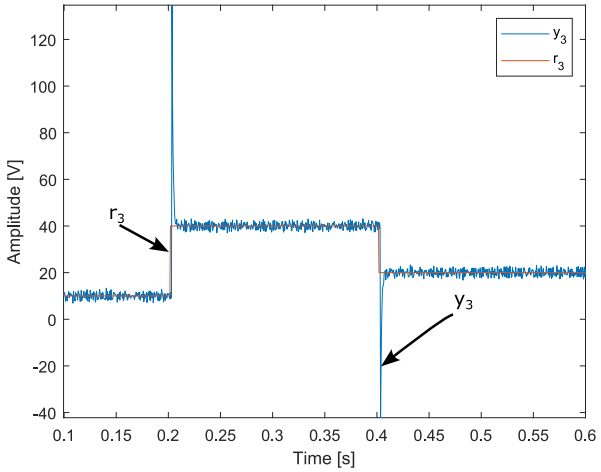

Fig. 11. Output v_3 tracking response of the third segment of the microgrid under noise conditions

A similar evaluation is performed by considering the proposed approach with dead beat closed loop dynamics. In Fig. 12 is presented the output response v_1 for reference tracking by using the proposed approach with dead beat closed loop dynamics.

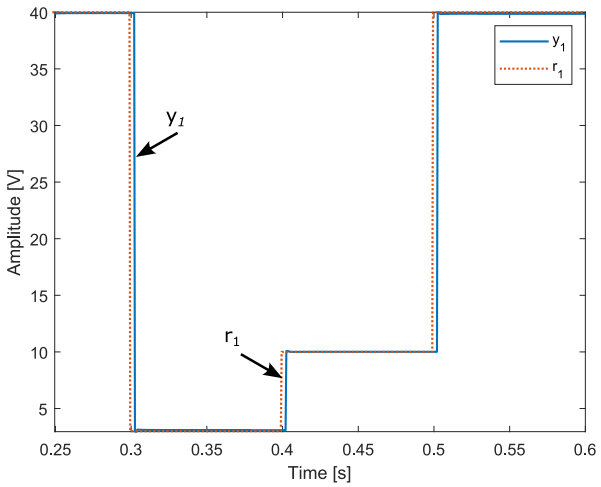

Fig. 12. Output v_1 considering reference tracking in the microgrid for the proposed approach closed loop dead beat dynamics

In Fig. 13 is presented the control signal for reference tracking response shown in Fig. 12.

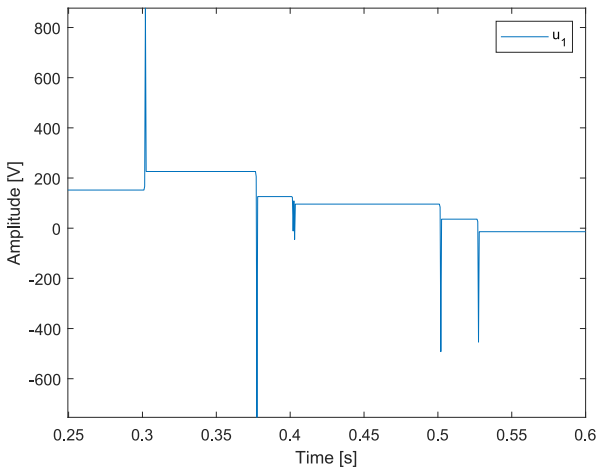

Fig. 13. Control signal for transfer function H_{11} of the microgrid

In Fig. 14 is presented the output response v_2 for reference tracking by using the proposed approach with dead beat closed loop dynamics.

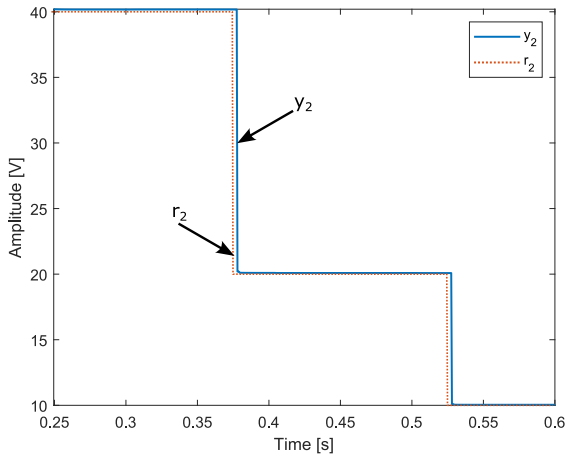

Fig. 14. Output v_2 considering reference tracking in the microgrid for the proposed approach closed loop dead beat dynamics

In Fig. 15 is presented the control signal for reference tracking response shown in Fig. 14.

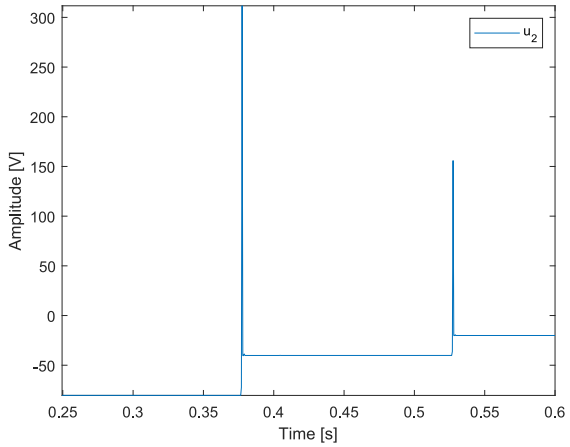

Fig. 15. Control signal for transfer function H_{22} of the microgrid

In Fig. 16 is presented the output response v_3 for reference tracking by using the proposed approach with dead beat closed loop dynamics.

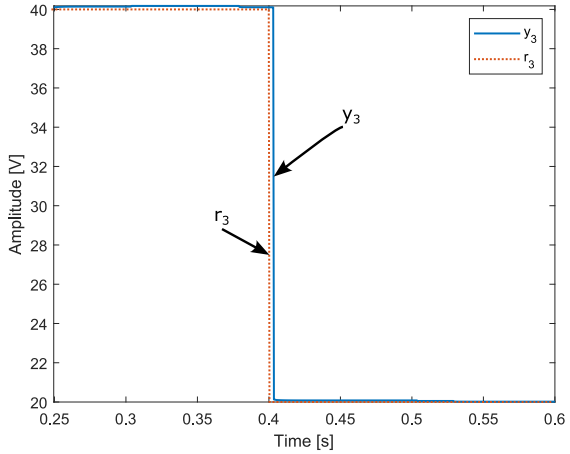

Fig. 16. Output v_3 considering reference tracking in the microgrid for the proposed approach closed loop dead beat dynamics

In Fig. 17 is presented the control signal for reference tracking response shown in Fig. 16.

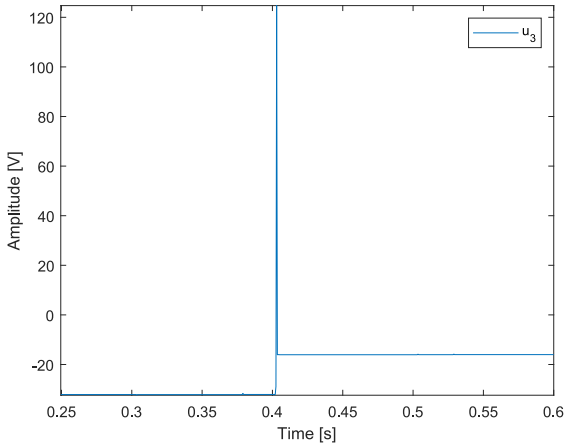

Fig. 17. Control signal for transfer function H_{33} of the microgrid

A similar evaluation is performed for a simulation of the microgrid under 10% additive output noise environment. In Fig. 18 is presented the output v_1 for the first segment of the microgrid.

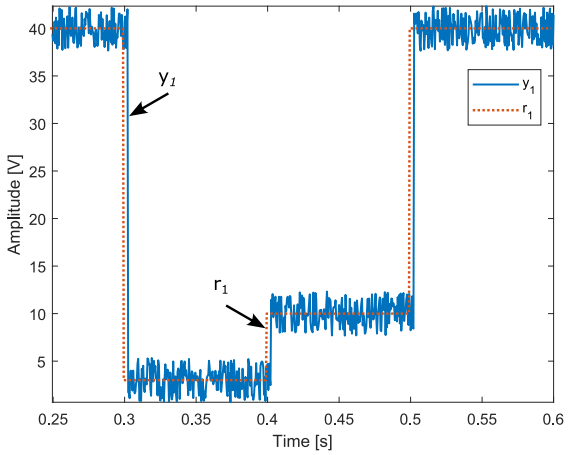

Fig. 18. Tracking response for the first segment of the microgrid with additive noise

In Fig. 19 is presented the corresponding control signal of tracking response presented for the first segment of the microgrid in Fig. 18.

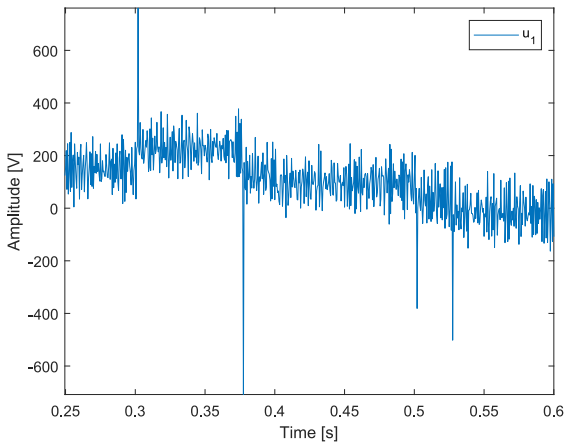

Fig. 19. Control signal for the first segment of the microgrid with additive noise

In Fig. 20 is presented the output v_2 for the second segment of the microgrid.

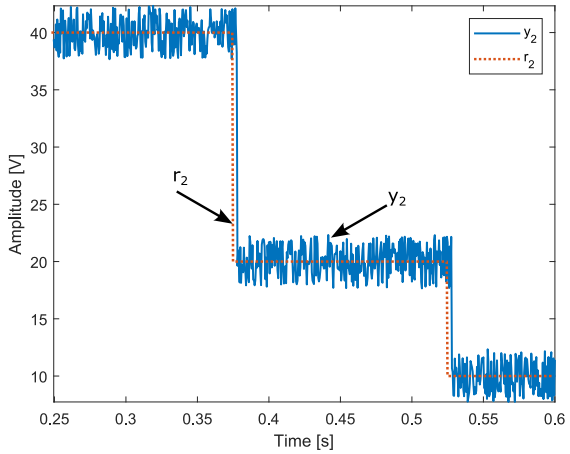

Fig. 20. Tracking response for the second segment of the microgrid with additive noise

In Fig. 21 is presented the corresponding control signal of tracking response presented for the second segment of the microgrid in Fig. 20.

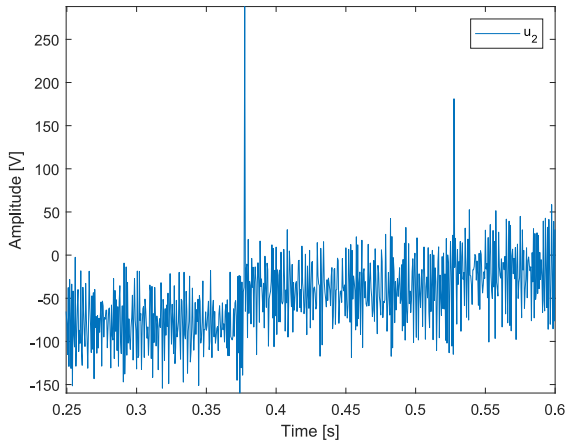

Fig. 21. Control signal for the second segment of the microgrid with additive noise

In Fig. 22 is presented the output v_3 for the third segment of the microgrid.

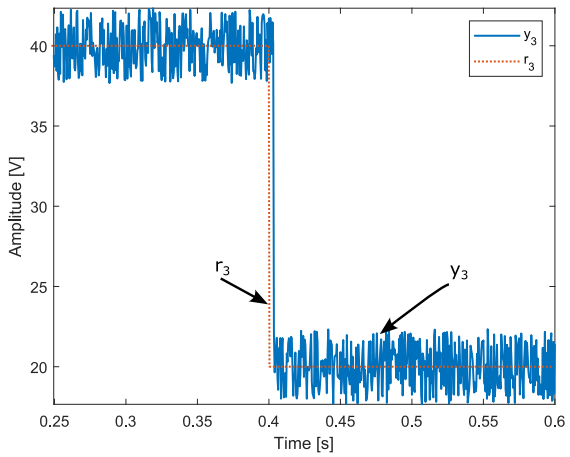

Fig. 22. Tracking response for the third segment of the microgrid with additive noise

In Fig. 23 is presented the corresponding control signal of tracking response presented for the third segment of the microgrid in Fig. 22.

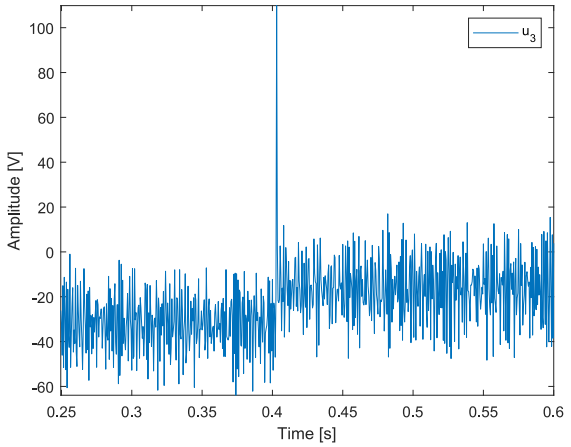

Fig. 23. Control signal for the third segment of the microgrid with additive noise

In Fig. 24 is presented the comparison for output y_1 for the proposed approach and a polynomial approach.

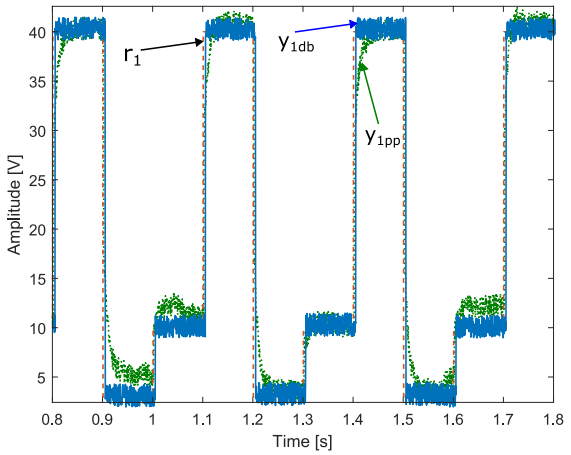

Fig. 24. Tracking response comparison of the proposed dead-beat approach y_{1db} for output y_1 and the polynomial pole-placement approach y_{1pp}

In Fig. 25 is presented the comparison for output y_2 for the proposed approach and a polynomial approach.

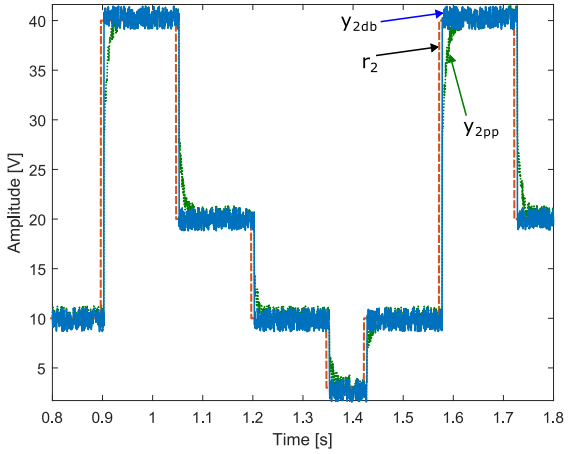

Fig. 25. Tracking response comparison of the proposed dead-beat approach y_{2db} for output y_2 and the polynomial pole-placement approach y_{2pp}

A comparison analysis with a polynomial pole-placement technique y_{kpp} is performed in comparison with the proposed adaptive sliding mode approach with dead-beat dynamics y_{kdb} with $k = 1, 2, 3$. In Fig. 26 is presented the comparison for output y_3 for the proposed approach and a polynomial approach.

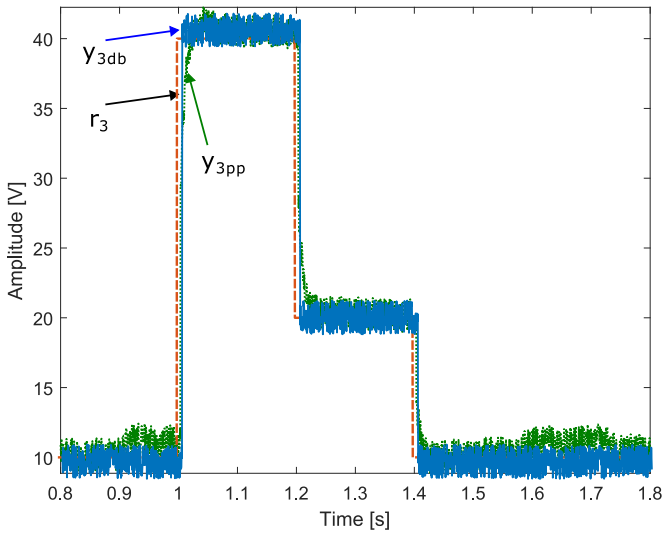

Fig. 26. Tracking response comparison of the proposed dead-beat approach y_{3db} for output y_3 and the polynomial pole-placement approach y_{3pp}

Finally, a evaluation of the proposed approach is performed by using the real time implementation based on a HIL structure. In Fig. 27 are shown the results of the evaluation of the proposed approach over the HIL implementation for each of the subsystems.

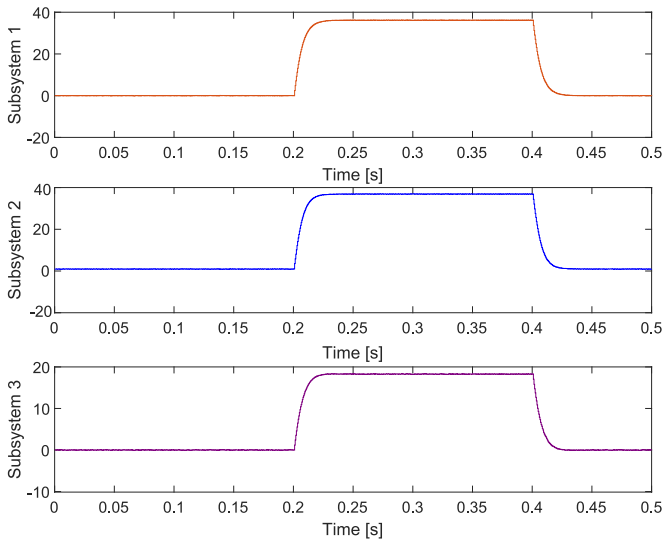

Fig. 27. Real time evaluation of the microgrid for outputs v_1, v_2 and v_3 corresponding to each subsystem

In Fig. 28, Fig. 29 and Fig. 30 are shown the results of the evaluation of the HIL implementation for each of the subsystems.

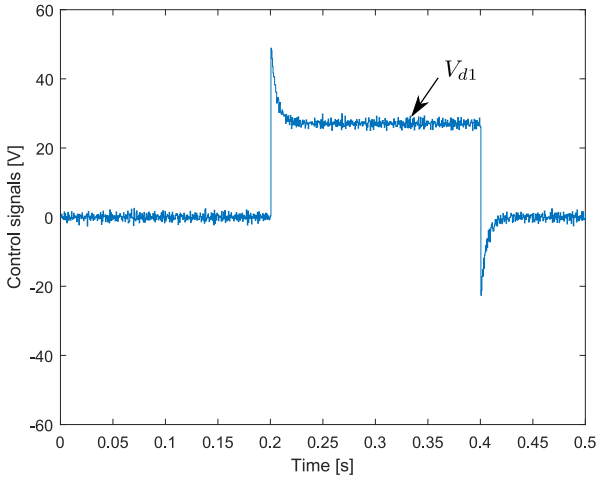

Fig. 28. Real time evaluation of the microgrid for input V_{d1}

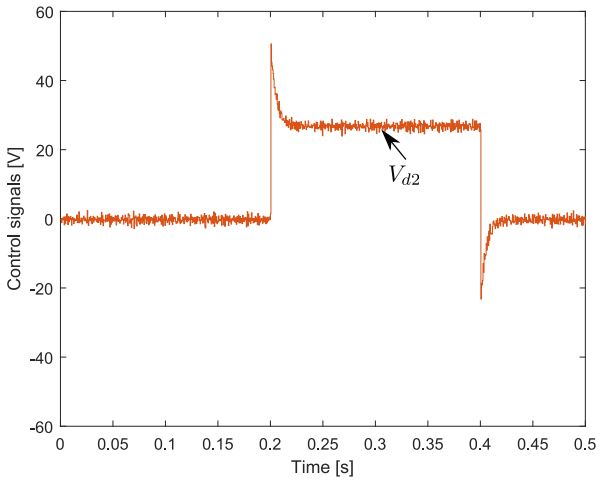

Fig. 29. Real time evaluation of the microgrid for input V_{d2}

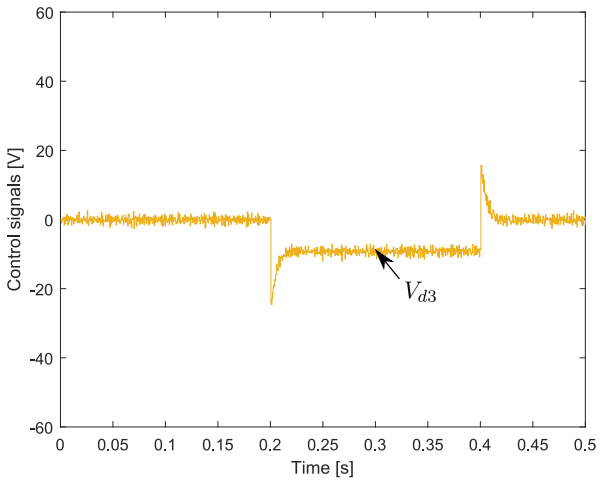

Fig. 30. Real time evaluation of the microgrid for input V_{d3}

IV. Conclusions

This work presents an adaptive control approach for sliding mode dynamics based on dead-beat criteria for stability in closed-loop. The proposed method is evaluated under simulation and real-time for a 3 inputs and 3 outputs microgrid. It is worth noting that the proposed approach adapts to the structure of the plant. Also, it can be seen that

the tracking performance is adequate for reference tracking even when the system parameters are identified during the tracking procedure. It is worth mentioning that the system is evaluated in simulation and in real-time by using a HIL structure. The proposed approach shows that the dead-beat stability in a closed-loop is guaranteed and validated under external disturbances corresponding to 10% additive noise.

REFERENCES

[1] A. Trebi-Ollennu, B. Stacey, and B. White, "A multivariable decoupling design of an rov depth control system: a direct adaptive fuzzy smc approach," in *Proceedings of 1995 American Control Conference - ACC'95*, vol. 5, 1995, pp. 3244–3248 vol.5.

[2] L.-R. You, Z.-Y. Ma, X.-H. Wang, and H. Zhang, "Sliding mode control for permanent-magnet synchronous motor based on a double closed-loop decoupling method," in *2005 International Conference on Machine Learning and Cybernetics*, vol. 2, 2005, pp. 1291–1296 Vol. 2.

[3] G. Guoqin, D. Qinqin, and W. Wei, "Sliding mode control of parallel robot by optimizing switching gain based on rbf neural network," in *Proceedings of the 31st Chinese Control Conference*, 2012, pp. 975–980.

[4] S.-X. Hou and X.-G. Zhang, "Multi-variable continuous higher-order sliding mode control for pmsm," in *2018 Chinese Control And Decision Conference (CCDC)*, 2018, pp. 3732–3737.

[5] V. Repecho, J. B. Waqar, D. Biel, and A. Dòria-Cerezo, "Zero speed sensorless scheme for permanent magnet synchronous machine under decoupled sliding-mode control," *IEEE Transactions on Industrial Electronics*, vol. 69, no. 2, pp. 1288–1297, 2022.

[6] X. Liu, C. Yang, Z. Che, and L. Zhou, "A novel equivalent input disturbance-based adaptive sliding mode control for singularly perturbed systems," *IEEE Access*, vol. 9, pp. 12 463–12 472, 2021.

[7] A. Derdiyok, "Speed-sensorless control of induction motor using a continuous control approach of sliding-mode and flux observer," *IEEE Transactions on Industrial Electronics*, vol. 52, no. 4, pp. 1170–1176, 2005.

[8] P. C.-P. Chao and C.-Y. Shen, "Sensorless tilt compensation for a three-axis optical pickup using a sliding-mode controller equipped with a sliding-mode observer," *IEEE Transactions on Control Systems Technology*, vol. 17, no. 2, pp. 267–282, 2009.

[9] F. Osorio-Arteaga, J. J. Marulanda-Durango, and E. Giraldo, "Robust multivariable adaptive control of time-varying systems," *IAENG International Journal of Computer Science*, vol. 47, no. 4, pp. 605–612, 2020.

[10] M. H. Saeed, W. Fangzong, B. A. Kalwar, and S. Iqbal, "A review on microgrids' challenges amp; perspectives," *IEEE Access*, vol. 9, pp. 166 502–166 517, 2021.

[11] M. Bueno-Lopez and E. Giraldo, "Real-time fractional order pi for embedded control of a synchronous buck converter," *Engineering Letters*, vol. 29, no. 3, pp. 1212–1219, 2021.

[12] K. N. N. A. Kumar and C. P. Kurian, "Model based control using c2000 microcontroller," in *2014 International Conference on Advances in Energy Conversion Technologies (ICAECT)*, 2014, pp. 13–20.

[13] M. Bueno-Lopez and E. Giraldo, "Real-time decentralized control of a hardware-in-the-loop microgrid," *IAENG International Journal of Computer Science*, vol. 48, no. 3, pp. 653–662, 2021.

[14] S. Huseinbegovic, B. Perunicic-Drazenovic, B. Veselic, and C. Milosavljevic, "Higher order sliding mode based dead-beat control with disturbance compensation for multi-input lti systems," in *2018 15th International Workshop on Variable Structure Systems (VSS)*, 2018, pp. 309–314.

[15] D. Giraldo and I. Tabares, "A digital adaptive control," in *Proceedings of IFAC/IFIP Conference on Management and Control of Production and Logistics*, vol. 2, 1997, pp. 720–725.

[16] Y. Chen, D. Sun, B. Lin, T. W. Ching, and W. Li, "Dead-beat direct torque and flux control based on sliding-mode stator flux observer for pmsm in electric vehicles," in *IECON 2015 - 41st Annual Conference of the IEEE Industrial Electronics Society*, 2015, pp. 002 270–002 275.

[17] G. C. Goodwin and K. S. Sin, *Adaptive Filtering, Prediction and Control*. Englewood-Cliffs: Dover Publications Inc., 2009.

[18] S. Sarpturk, Y. Istefanopulos, and O. Kaynak, "On the stability of discrete-time sliding mode control systems," *IEEE Transactions on Automatic Control*, vol. 32, no. 10, pp. 930–932, 1987.

[19] O. Jedda and A. Douik, "Discrete-time sliding mode control for an inverted pendulum system," in *2018 International Conference on Advanced Systems and Electric Technologies (ICASET)*, 2018, pp. 272–276.

[20] M. L. Corradini, "A robust sliding-mode based data-driven model-free adaptive controller," *IEEE Control Systems Letters*, vol. 6, pp. 421–427, 2022.